DEVELOPMENT, SKIN TARGETING AND ANTIFUNGAL EFFICACY OF TOPICAL LIPID NANOPARTICLES CONTAINING ITRACONAZOLE

JULIA SAPIENZA PASSOS[1,2], LUIZA CAPELLO DE MARTINO[1,2], VANESSA FRANCO CARVALHO DARTORA[1], GABRIEL L. B. DE ARAUJO[2], KELLY ISHIDA[1], LUCIANA B. LOPES[1]

[1] Institute of Biomedical Sciences, University of São Paulo, São Paulo, SP, Brazil

[2]School of Pharmaceutical Sciences of São Paulo, University of São Paulo, São Paulo, SP, Brazil

Corresponding author:
Luciana B. Lopes, PhD

Department of Pharmacology, Institute of Biomedical Sciences

University of São Paulo

Av. Prof. Lineu Prestes 1524, São Paulo - SP, Brazil

lublopes@usp.br

phone: 55 11 3091-7317

Abstract.

Considering the increased incidence of sporotrichosis and other fungal infections in rural and urban areas, and the limitations and adverse effects of oral itraconazole therapy, we studied nanostructured lipid carriers (NLC) as topical delivery systems to increase itraconazole localization in skin lesions and associate efficacy with reduced systemic exposure. Unloaded and itraconazole-loaded NLC showed nanometric size (~216-340 nm), negative zeta potential (~ -17 mV), and high entrapment efficiency (~97%). NLC treatment decreased transepidermal water loss, an index of cutaneous barrier function, in intact skin and in tissues damaged with a linear incision (to mimic lesions) by 23-36%, and reduced drug transdermal delivery by ~2-fold, demonstrating its ability to localize itraconazole within the skin. The unloaded and itraconazole-loaded NLC were considered safe, as indicated by scores of 0.5 and 0.6 in HET-CAM models, respectively, and lack of toxicity (measured by survival and health index) on the *Galleria mellonella* larvae. The values obtained for minimum inhibitory concentration and minimum fungicidal concentration on *Sporothrix brasiliensis* yeasts were 0.25 and 32 μg/mL, respectively. The drug in solution displayed similar values, indicating that encapsulation does not hinder itraconazole antifungal effect. NLC treatment improved the survival rate and health index of *G. mellonella* larvae infected with *S. brasiliensis* yeasts and *C. albicans*, demonstrating antifungal efficacy. Taken together, itraconazole encapsulation in NLC represents a viable strategy to optimize cutaneous localization without compromising its efficacy against fungal infections.

Key words: itraconazole, skin, topical, nanostructured lipid carriers, nanoparticle, sporotrichosis

1. Introduction

Sporotrichosis is a subcutaneous mycosis with a worldwide distribution caused by the thermodimorphic fungi *Sporothrix* spp., which affects humans and other animals. This mycosis has several clinical manifestations, including skin lesions that can rapidly evolve to a disseminated form in immunocompromised individuals (Almeida-Paes et al., 2014). Historically, this fungal infection has been associated with agricultural work, since the fungus is found in decomposing soil or plants. However, zoonotic transmission is possible, and occurs mainly by traumatic inoculation due to scratching or biting of infected animals. Among *Sporothrix* spp., *Sporothrix brasiliensis* is related to the zoonotic sporotrichosis epidemic by cats in Brazil, and the high transmission potential for humans is one of the factors that generates concern around the disease, which today is considered one of the main infectious diseases caused by animals (Almeida-Paes et al., 2014; Friedman and Schwartz, 2019) (Silva et al., 2012). Since 1998, an increase in the number of cat-transmitted cases of human sporotrichosis in Rio de Janeiro state has been detected, especially in its capital metropolitan region. Between 1995 and 2015, approximately 4000 cases were reported in the state, a pronounced increase compared to the 1848 cases diagnosed from 1997 to 2007 (Gremião et al., 2017; Silva et al., 2012). However, this number might be underestimated since sporotrichosis became a compulsory notifiable disease only in 2013 (Alzuguir et al., 2020).

The current protocol for sporotrichosis therapy, even for the cutaneous form, is based on oral administration of itraconazole (Kauffman et al., 2007). The pharmacological mechanism of action of itraconazole involves the inhibition of the P450-dependent lanosterol C14α- demethylase enzyme, which is an essential step for the conversion of lanosterol to ergosterol in the fungus, leading to the disruption of permeability and function of the plasma membrane (Vanden Bossche et al., 1995). However, itraconazole is a poorly water-soluble drug, and presents low gastrointestinal absorption when administered orally, varying with dose and time (Kumar and Goindi, 2014). Its systemic use is associated with several adverse effects, including abdominal pain and headache, and

is contraindicated in patients with renal and hepatic insufficiency (Kumar and Goindi, 2014; Miller et al., 2008). In addition to being subject to first-pass intestinal and hepatic metabolism, itraconazole is a potent inducer of cytochrome P450 enzymes, and interferes with the metabolism and clinical efficacy of various drugs, including simvastatin and omeprazole (Quinney et al., 2008). This effect may also lead to long-term treatment discontinuation due to increased liver enzymes (Gilaberte et al., 2014). Formulation and administration of itraconazole are further complicated by its poor aqueous solubility, which makes the development of a sufficiently bioavailable itraconazole formulation challenging. Therefore, topical administration of itraconazole could circumvent these problems, maximizing drug efficacy in cutaneous and subcutaneous lesions and reducing undesirable systemic adverse effects. Despite the potential advantage of topical delivery, there are no clinically available formulations for this route.

Among the various topical delivery systems developed for lipophilic drugs, nanostructured lipid carriers (NLC) present many interesting features, including the ability to (i) increase chemical stability of the drug, (ii) maintain skin hydration, (iii) prolong drug release, and (iv) provide greater entrapment efficiency of lipophilic drugs due to the presence of liquid lipids in the matrix (Pardeike et al., 2009; Souto and Muller, 2008). As far as topical administration is concerned, protection against degradation and formation of a drug depot in the skin, which can provide prolonged drug release, contribute to drug localization in lesions and reduce the administration frequency, represent the main advantages of these systems (Das et al., 2012) (Pardeike et al., 2009).

In light of the aforementioned concepts, this paper reports the development and characterization of NLC for itraconazole incorporation and topical delivery as an alternative for localized treatment of sporotrichosis cutaneous lesions. After formulation characterization, parameters such as drug cutaneous deposition and transport, irritation potential and antifungal activity of the nanocarrier were investigated.

2. Material

Polysorbate 80 (Tween 80), sorbitan oleate (Span 80), poloxamer 188 (Pluronic F-88), itraconazole, sodium hydroxide and propylene glycol were obtained from Sigma (St. Louis, MO, USA). Tricaprylin was kindly supplied by Abitec Corporation (Janesville, WI, USA), and glyceryl behenate (Compritol 888) from Gatefosse (Saint-Priest, France). Acetonitrile, ethanol and methanol were purchased from Mallinckrodt Baker (Phillipsburg, NJ, USA). Ultra-pure water was used unless stated in the individual methods.

3. Methods

3.1. Nanocarrier development and optimization

Various ratios of solid and liquid lipids were used to obtain the nanocarriers since their proportion is determinant for the physicochemical characteristics of NLC. Tricaprylin and Compritol 888 (glyceryl behenate) were selected as liquid and solid lipids, respectively, and a lipophilic surfactant (Span 80) was added to this oil phase. After melting, the aqueous phase (1% poloxamer 188 solution containing polysorbate 80) was added to the oil phase under vortex stirring, and the final mixture was sonicated for 20 minutes in pulses (50s on and 30s off) in a water bath at room temperature using 40% amplitude (VCX500, Sonics, Newtown, CT). Few modifications were included in this general protocol to assess the influence of oil phase content and surfactant concentration on the characteristics of the nanocarriers.

The influence of surfactant concentration on nanoparticle characteristics was studied using a 2^2 factorial test, in which two variables (hydrophilic and lipophilic surfactant represented by Tween 80 and Span 80, respectively) were studied and each one was divided into two sub-levels (two concentrations, 3 and 1.5%). The influence of the ratio between solid and liquid lipids was also studied by mixing these components at 7:3, 5:5 or 3:7 (w/w).

Itraconazole was incorporated into the nanocarrier oil phase mixture to obtain final concentrations ranging from 1 to 5% (w/w in regards to the total formulation). Our goal was to maximize the concentration of itraconazole without disrupting nanocarrier formation.

The efficiency of itraconazole encapsulation in the NLC was evaluated indirectly by the ultrafiltration method. First, 300 µL aliquot of the nanoparticle dispersion was suspended in distilled water (1:2, v/v). Dilution was necessary to facilitate ultrafiltration and centrifugation; undiluted samples did not yield a filtrate most likely because of viscosity. The samples were placed in the upper chamber of an Amicon Ultra 4 centrifugal filter (Millipore Corporation, USA), and centrifuged for 1 hour and 30 min at 4000 rpm (Eppendorf, mod. 5430R, Hamburg, Germany). The filtrate was collected for itraconazole quantification by fluorescence, and entrapment efficiency (EE%) was calculated using Equation 1 (Cirri et al., 2018).

$$EE\% = \frac{W_{initial\ drug} - W_{free\ drug}}{W_{initial\ drug}} \times 100 \quad \text{(Equation 1)}$$

where $W_{initial\ drug}$ is the initial drug amount used for NLC preparation and $W_{free\ drug}$ the amount of free drug detected in the filtrate.

3.2. Physicochemical characterization of selected nanocarrier properties

Size, polydispersity index and zeta potential were determined using Zetasizer NanoZS90 equipment (Malvern, UK) after nanocarrier dilution with water at 1:100 (w/w).

The structure and morphological aspects of the nanocarriers were assessed using scanning electron microscopy (SEM) and transmission electron microscopy (TEM). For SEM, one drop of unloaded nanocarrier diluted with distilled water at 1:1000 (w/w) was placed in a glass coverslip previously covered with 10 µL of a poly-L-Lysine solution (1 mg/mL) for 30 minutes and rinsed. Prior to observation, the samples were dried at room temperature for 24 h, mounted onto aluminum stubs for metallization with platinum, and examined using a Quanta FEG 450 scanning electron microscope (FEI Company, Hillsborough, OR, USA) at the core facility of the Polytechnic School, University of São Paulo. For TEM, samples were contrasted with 2% phosphotungstic acid, and adsorbed onto carbon film on 300 mesh copper grids and dried at room temperature for 24 h prior to observation in a transmission electron microscope Tecnai FEI G20 XTWIN (FEI Company, Hillsborough, OR, USA) at the Institute of Biomedical Sciences, University of São Paulo.

3.3. Thermal analysis

To learn more about drug solubilization in the nanocarrier and to assess the influence of the liquid lipid on the solid lipid crystallinity, the thermal behavior of the selected nanocarrier was assessed by differential scanning calorimetry (DSC) and thermogravimetric analysis (TG), using DSC 7020 equipment (Hitachi High Technology Corporation, Tokyo, Japan). Both unloaded and itraconazole-loaded nanocarriers (at 1%) were dried under vacuum (FreeZone 2.5, Labconco, Kansas City, MO, USA) for 24 h before analysis. In addition, the solid lipid and itraconazole were also analyzed individually.

In thermogravimetric analysis, samples of 5 mg were placed in platinum pans and submitted to measurements at a heating range of 30 to 600 °C at 10 °C/min, without isotherm. DSC was performed with samples of 2 mg, placed in partially closed aluminum pans, in a temperature range of 25 to 300 °C at 10 °C/min, with 3 min isotherm at 25°C. Nitrogen was used as a purge gas (100 mL/min) in both analyses.

3.4. Evaluation of NLC irritation potential

In order to evaluate the irritation potential of NLC, Hen's Egg Test - Chorioallantoic Membrane (HET-CAM) was performed. The protocol was conducted in accordance with the guidelines from the Brazilian Council for Control of Animal Experimentation (CONCEA) and approved by the Animal Care and Use Committee (IACUC) at the Institute of Biomedical Sciences of the University of São Paulo.

Fertilized chicken eggs (Leghorn breed) were incubated for 9 days at 37 ± 0.5 °C and 70% humidity (Premium Ecologica, Belo Horizonte, MG, Brazil) with automatic rotation every 2 h. CAM was exposed and treated for 5 minutes with unload and itraconazole-loaded NLC (0.1 mL), saline solution (negative control) and NaOH (0.1 M, positive control). The membranes were photodocumented (Nikon, SMZ 1500, Tokyo, Japan) before, during and after treatment. Each

treatment was performed in 3-5 eggs and the development of hemorrhage, vascular lysis and coagulation was evaluated within 1 to 5 min after application. According to the reaction time, the irritation score was calculated, which allows the formulation to be classified from non-irritant to severe irritant, according to Equation 2, as previously described (McKenzie et al., 2015; Migotto et al., 2018):

$$Score = \left(\left(301 - \left(\frac{Ht}{300}\right)\right) \times 5\right) + \left(\left(301 - \left(\frac{Lt}{300}\right)\right) \times 7\right) + \left(\left(301 - \left(\frac{Ct}{300}\right)\right) \times 9\right) \quad \text{(Equation 2)}$$

where *Ht*, *Lt* and *Ct* are hemorrhage, lysis, and coagulation time, respectively.

3.5. Stability study of nanocarriers

The physicochemical stability of selected NLCs were studied by macroscopic and microscopic observation taking into consideration the breakdown of the system, due to coalescence and/or gravitational separation, and analysis of particle size, polydispersity index and zeta potential.

In conical tubes, 0.5g of the selected NLC (prepared in triplicate) were stored at room temperature (25 °C) and formulation evaluation was performed at days 0 (immediately after production), 7, 15, 30, 45, 60 and 90 days after dilution with water (1:100 v/v). Physicochemical stability of the itraconazole-loaded nanocarrier (1%) was also investigated at 0, 30, 60 and 90 days.

3.6. Nanocarrier influence on the cutaneous barrier and skin penetration

3.6.1. Skin model

Porcine ears (obtained from a local slaughterhouse) were rinsed with water, and after drying, a split was performed using a scalpel to separate the skin and cartilage from the ear; subsequently, excess hair and subcutaneous tissue were removed with scissors and scalpel. The skin pieces were sectioned, wrapped in aluminum foil and stored frozen at -80 °C. On the day of the experiment, the skin was thawed and pinned to the surface of a styrofoam block (with the stratum corneum facing

up), and layers of 0.5 mm thickness were obtained using a 75mm dermatome (Nouvag AG, Goldach, Switzerland), which were assembled on the diffusion cells.

We employed intact skin and tissues subjected to a linear incision to simulate barrier impairment. Using a scalpel blade under a stereomicroscope, a linear incisional wound was created to expose all skin layers without perforating the tissues (Ng et al., 2017). We acknowledge that this model does not mimic the complex structure of sporotrichosis lesions, but it enabled us to investigate differences on the nanocarrier-mediated changes on the transepidermal water loss, skin retention and percutaneous permeation of itraconazole when the skin barrier was compromised.

3.6.2. Transepidermal water loss

Skin sections were mounted in Franz diffusion cells (Hanson, Chatsworth, USA) with the stratum corneum facing the donor compartment and dermis facing the receptor compartment, which was filled with phosphate buffered saline maintained at 37.0 ± 0.5°C with magnetic stirring at 350 rpm throughout the experiment.

The skin sections (intact or subjected to a linear incision) were treated with the selected nanocarrier for up to 24 h, by transferring 200 μL of the nanocarrier dispersion to the donor compartment of diffusion cells. Transepidermal water loss (TEWL) was measured with a closed chamber evaporimeter (Vapometer, Delfin Technologies Ltd., Kuopio, Finland) with an adaptor to fit the diffusion cell opening before treatment (allowing 15 minutes for equilibration) and at 24 h post-treatment, before and after removing the formulation. The later was performed as follows: the formulation was removed by wiping the skin surface with humid tissue paper, the skin sections were reassembled in the diffusion cells and equilibrated for 20 min before TEWL measurement as previously described (Carvalho et al., 2017a; Carvalho et al., 2017b). Results were expressed as Δ transepidermal water loss, calculated as the difference between transepidermal water loss values before and after treatment, and compared to those obtained with water, used as a negative control.

3.6.3. Skin penetration of itraconazole

Skin penetration of itraconazole was assessed using Franz diffusion cells and porcine ear skin as model tissue as previously described in item 3.6.2, excepted that the receptor phase was composed of water (pH=4 with phosphoric acid), containing 20% ethanol to improve drug solubility from less than 0.5 μg/mL to over 20 μg/mL.

In the donor compartment of the diffusion cell, the selected NLC was added and left in contact with the skin for 6 or 24 h; a drug solution of propylene glycol (1% w/w) was used as control formulation. At the end of the experiment, the tissue samples were rinsed with distilled water to remove excess formulation, and the stratum corneum was separated from the rest of the skin using 15 pieces of adhesive tapes (tape stripping technique). The first piece was discarded and the others were added to a conical tube (containing methanol as extracting solvent). The remainders of the skin (epidermis without stratum corneum and dermis, ED) were cut into small pieces and placed in tubes containing methanol. Itraconazole was extracted from the tapes and from skin pieces with methanol using a hand-held tissue homogenizer and bath sonication (15 min), prior to fluorimetry quantification.

3.6.4. Visualization of NLC-mediated skin penetration

To better understand NLC-promoted drug penetration and distribution in the skin, rhodamine B (0.5%, w/w) was used as a fluorescent marker, replacing itraconazole in the nanocarrier. Rhodamine B-loaded NLCs were prepared as previously described in session 3.1 and the skin penetration was evaluated after 6 h in skin sections subjected to a linear incision. After treatment, the tissue samples were rinsed with distilled water, cut into small sections and mounted on glass slides. The slide with upward facing stratum corneum was observed under LSM780 confocal microscope system at the CEFAP core facility (Institute of Biomedical Sciences, University of São Paulo, Carl Zeiss Meditec AG, Oberkochen, Germany). The depth analysis was executed by ZEN lite Software (Carl Zeiss Meditec AG, Oberkochen, Germany).

3.7. Itraconazole quantification

Fluorimetric analyses were performed using a multifunctional microplate reader (SpectraMax M5, Molecular Devices, USA) using excitation and emission at 264 and 380 nm, respectively (Srivatsan et al., 2004). For the analysis of the samples, itraconazole calibration curves were constructed in the extracting solvent in the range of 0.2-100 μg/mL. Also, to determine whether matrix components interfere with the quantification method, untreated skin samples were subjected to the same drug extraction procedure and analyzed; no interference with the quantification method was observed.

3.8. Influence of encapsulation on antifungal effect

To evaluate the influence of itraconazole encapsulation on its antifungal activity, the minimum inhibitory concentration (MIC) was determined by the broth microdilution technique (CLSI, 2008). As positive control, free itraconazole, fluconazole and amphotericin B were used. Drugs and nanocarriers were serially diluted 1:2 (v/v) in 0.16 M MOPS buffered RPMI 1640 medium in a 96-wells microplate. The fungal inoculum of yeasts from *S. brasiliensis* (Sb54 strain from cutaneous lesion of feline sporotrichosis) or *Candida albicans* (SC5314), standardized at 5 x 10^3 CFU/mL, was dispersed in each well and the microplates incubated at 35 °C for 120 h and 48 h, respectively. *C. albicans* was used as a proof of concept for antifungal efficacy because it is more virulent than the *S. brasiliensis* (Sb54) strain employed. The lowest antifungal concentrations that inhibit 50% fungal growth (MIC) were defined by determination of optical density at 492 nm for antifungals and semi-quantitative inverted microscope analysis (Bioval XDS-1) for nanocarriers, since turbidity hampered absorbance measurement. The minimum fungicidal concentration (MFC), defined as the lowest concentration of drugs that killed 99.9% of fungal cells, was determined by incubation onto a Petri dish containing free-drug Sabouraud dextrose agar of a 10 μL aliquot of wells where there was no growth in MIC experiments. The effect was considered fungicidal when MFC was ≤ 4xMIC (Espinel-Ingroff et al., 2002).

Prior to performing the antifungal activity evaluation of the nanocarriers, the toxicity of unloaded and itraconazole-loaded NLC was evaluated using non-infected *Galleria mellonella* larvae. Healthy larvae (2.0 to 2.5 cm in length) were selected and divided into experimental groups of 20 larvae. An aliquot of 10 µL of unload or itraconazole-loaded NLC (diluted 1:4 in PBS or 125 mg/kg of itraconazole) was administered in the last pro-leg of the larvae and incubated at 37 °C (Spadari et al., 2019). Survivor counts and health status were performed daily up to 5 days to construct larval survival curves, as described in the literature (**Supplementary Table 1**) (Champion et al., 2018).

Subsequently, *G. mellonella* larvae were infected with 10 µL of yeasts inoculum (1 x 10^9 CFU/mL for *S. brasiliensis* and 5 x 10^7 CFU/mL for *C. albicans*) in the last left pro-leg with the aid of Hamilton syringes (Frenkel et al., 2016). After 30 min, the last right pro-leg was used to antifungal treatments with unloaded and itraconazole-loaded nanostructured lipid carriers and compared with itraconazole dispersion in PBS, both at doses of 20 and 40 mg/kg of itraconazole. To prepare the dispersion, itraconazole was dissolved in DMSO, and this solution was diluted in PBS immediately before administration (up to 1% DMSO in the final PBS solution) to enable administration of 20 or 40 mg/Kg of itraconazole. The larvae were incubated at 37ºC in Petri dishes and observed daily up to 5 days for survivor counts and health status (Champion et al., 2018).

3.9. Statistical analyses

The results are reported as means ± standard deviation. Data were statistically analyzed using t test or ANOVA (Tukey post-test) depending on the comparison to be performed (GraphPad Prism software). Values were considered significantly different when $p<0.05$.

4. Results

4.1. Obtainment of the nanostructured lipid carriers (NLC)

The first goal of the present study was to develop a nanostructured lipid carrier for increasing itraconazole localization in sporotrichosis skin lesions. The influence of the ratio between solid and liquid lipids, surfactant and itraconazole concentration on nanocarrier formation and physicochemical characteristics were assessed (**Table 1**).

An essential condition for obtaining NLC is that the particles remain solid at room temperature (Chen et al., 2017; Pardeike et al., 2009). Thus, different ratios of solid and liquid lipids were investigated, and it was observed that, although ratios of 9:1 - 3:7 (w/w, solid:liquid lipids) remained solid, only proportions greater than or equal to 5:5 (w/w) resulted in nanoparticles with polydispersity index (pdi) $\leq$ 0.25 (which suggests low polydispersity) (Danaei et al., 2018). All particles were negatively charged (-17.3 to -18.4 mV), which is consistent with efficient antifungal carriers previously studied (Pinto Reis et al., 2016; Spadari et al., 2019) Due to the nanometric size (225.5 nm) and lower pdi (0.19) values, the 5:5 ratio was selected. These results were obtained using Tween 80 and Span 80 (both at 5%) as hydrophilic and lipophilic surfactants, respectively, but in an effort to reduce surfactant content to decrease the irritation potential of the system while maintaining these suitable characteristics (Pepe et al., 2013), the effect of smaller concentrations (1.5 - 3%) of surfactants on size and pdi was studied.

Using Span 80 and Tween 80 at 1.5% resulted in particles of 289.6±8.1 nm and pdi of 0.33±0.03, which is not consistent with low polydispersity. Increasing Span to 3% did not largely affect pdi, whereas Tween at 3% reduced pdi to 0.24, suggesting a more pronounced effect of Tween 80 on size distribution. When both surfactants were employed at 3%, a significant reduction ($p < 0.05$) on size and pdi was observed compared to 1.5%, which prompted us to select this concentration for optimized nanocarriers; zeta potential was not largely affected.

Subsequently, the optimized nanocarrier was subjected to a short-term stability study to assess variations in the particle size, pdi and zeta potential as a function of time. Small variations (< 2-fold) in these parameters were set as minimum requisites for NLC use in further studies. The diameter and zeta potential changed less than 1.4 fold over 90 days, while the pdi did not exceed 0.3

(**Figure 1**). Furthermore, no phase separation, creaming or sedimentation was observed in the system throughout the study, suggesting that the selected NLC present the minimum requisites.

4.2. Itraconazole incorporation and influence on NLC characteristics

After selecting NLC composition and verifying its short-term stability, itraconazole was incorporated at various concentrations (1-5%) and the physicochemical characteristics of the nanocarrier were evaluated. Itraconazole increased NLC size by approximately 1.6 to 2.4-fold depending on concentration (**Figure 2A**). Low solubilization and presence of a white precipitate was observed in samples containing itraconazole at 3% or more within 24 h, suggesting that part of the drug was not incorporated in the nanoparticles. In addition, at 5% itraconazole increased values of particle size and pdi more than twice compared to the unloaded NLC. We selected the 1% concentration, and investigated its physicochemical stability for 90 days. Small increases in size (1.3-fold) and pdi (which remained below 0.4) were observed, but no signs of precipitation or phase separation were noticed during this period of time. The size of itraconazole-loaded NLC is in agreement with previous studies that employ nanoparticles for skin care and dermatological treatments (Gupta et al., 2013).

The entrapment efficiency of itraconazole in the lipid nanocarrier was 97.6± 1.8%, which is similar to previous studies of itraconazole-loaded lipid nanocapsules and NLCs for dermatological and pulmonary delivery (El-Sheridy et al., 2019; Pardeike et al., 2016).

Analysis of itraconazole-loaded NLC using transmission electron microscopy and scanning electron microscopy revealed well-dispersed nanoparticles with approximately spherical appearance, homogeneous distribution (**Figure 2 B and C**), and morphology similar to other lipid nanocarriers previously described (Bose et al., 2013). The particles visualized by TEM and SEM presented (in average) a diameter lower than 400 nm, which is in agreement with that determined by the light scattering technique.

4.3. Thermal behavior

Thermal analysis was conducted to gain more information about the stability, influence of lipid content in drug solubilization and crystallinity of the system. The TG curves revealed very stable compounds and absence of mass loss when materials were heated up to 300°C (**Figure 3A-D**).

DSC analysis of itraconazole indicated the presence of two endothermic signals, at approximately 85°C, which is believed to correspond to the formation of a nematic phase, and at 169°C, corresponding to the melting event (Parmentier et al., 2017; Six et al., 2003) (**Figure 3E** and **Table 2**). According to Six *et al.* the presence of this state would be beneficial in formulations, since it leads to better drug dissolution properties due to the decrease in the drug crystallinity (Six et al., 2003). Glyceryl behenate displayed a main endothermic event at 67-73°C (**Figure 3F**), which is in agreement with the melting point described by the manufacturer.

When glyceryl behenate was mixed with tricaprylin to form the nanoparticles, a decrease in the melting band to 58-65°C and on ΔH to 57.5 mJ/mg was observed (**Table 2**). These results suggest that, even though the liquid lipid reduced glyceryl behenate crystallinity at the ratio employed, the particles maintain the solid state for topical application (**Figure 3G**). A similar decrease in the glyceryl behenate melting event was also observed when itraconazole-loaded NLCs were analyzed; additionally, the signal corresponding to the nematic phase of itraconazole, but not of the main melting peak, was also present (**Figure 3H**).

4.4. Irritation potential

The HET-CAM assay was used to assess the nanocarrier irritation potential by evaluating the time-dependent occurrence of vascular toxicity endpoints (hemorrhage, lysis and coagulation) during five minutes following exposure. Although initially used to assess eye irritation, this method is now also employed for assessment of irritation to the skin and other tissues (Contri et al., 2016; Migotto et al., 2018; Mojeiko et al., 2019). While saline did not cause any noticeable change in the

membrane (**Figure 4**), the positive control (NaOH) caused lysis, bleeding and coagulation (resulting in a score of 17), which support their use as negative and positive controls, respectively (Carvalho et al., 2019). Both unloaded and itraconazole-loaded nanocarriers (at 1%) presented very few effects on the chorioallantoic membrane; some slight bleeding points were observed within 5 min post-treatment (marked with a black arrow in **Figure 4**), resulting in scores of 0.5 and 0.6, respectively and enabling their classification as non-irritant. According to these results, we do not expect the nanocarrier to generate further skin damage when applied to sporotrichosis lesions.

4.5. Evaluation of the nanocarrier influence on the skin barrier function and drug penetration

A representative histological image of the skin subjected to the linear incision (damaged skin) is represented in Figure **5A**. All skin layers were exposed by the incision, while maintaining part of the dermis intact.

To evaluate the nanocarrier ability to affect the barrier function of the skin, transepidermal water loss (TEWL) was measured. While the control (water) increased TWEL compared to values before treatment, NLC treatment decreased this parameter in intact and damaged skin by 23-36% (**Figure 5B**). These results suggest an occlusive effect on the skin, which is in agreement with previous studies that established a correlation between lipid concentration in the nanocarrier and skin hydration (Das et al., 2012). Even though the occlusive effect in intact skin has been reported before, our results build upon these observations demonstrating the ability of NLC to reduce TEWL in skin damaged with an incision.

Next, we evaluated the influence of the nanocarrier on itraconazole penetration in the stratum corneum (SC), epidermis without stratum corneum + dermis (ED) and in the receptor phase (RP, an index of percutaneous or transdermal delivery) after 6 and 24 h of drug treatment. Independent on the treatment (control solution or NLC) and skin condition (intact or with a linear incision), itraconazole was detected at larger amounts in the SC, suggesting the possibility of formation of drug depot in this skin layer even in the presence of an incision (**Figure 6**). The

control solution (propylene glycol 1%) and NLC delivered 93.0 ± 14.0 μg/cm^2 and 92.5 ± 1.3 μg/cm^2 of itraconazole into the SC of intact skin, respectively, after 6 h. A small increase in itraconazole delivery was observed at 24 h post-treatment (105.7 and 115.4 μg/cm^2, for control and nanocarrier respectively). Thus, compared with the control solution, the NLC did not provide significant increases in itraconazole penetration into SC at the studied periods of time. When it comes to drug delivery into ED, the nanocarrier reduced itraconazole penetration at 24 h, not at 6 h. More specifically, at 24 h, 59.7 ± 4.6 μg/cm^2 of itraconazole penetrated into the ED of intact skin from the solution, while the nanocarrier-mediated penetration was ~1.3-fold smaller.

As expected, the linear incision facilitated itraconazole penetration into and across the skin, and the amount of itraconazole that reached ED and RP after 24 h of treatment with the solution was ~1.5-1.9-fold higher compared to the intact tissue (**Figure 6**). Compared to the solution, the lipid nanocarrier promoted a 1.4-fold reduction in itraconazole penetration into ED ($p < 0.05$), and a ~2.0-fold reduction ($p < 0.01$) in the drug percutaneous permeation. The *skin/receptor phase* ratio resulting from NLC treatment was 17.0, (compared to a ratio of 9.2 resulting from treatment with the solution), demonstrating the NLC ability to improve cutaneous targeting.

To better understand the influence of NLC on skin penetration, and whether the penetration of the encapsulated compound is confined to the incision area or to cutaneous appendages, drug distribution in the damaged skin was studied using rhodamine B as a fluorescent marker. After administration of the rhodamine-loaded NLC for 6 h, tissue samples were analyzed by confocal microscopy. Fluorescence staining seemed to decrease with depth, even in the presence of the incision (**Figure 7 and Supplementary video 1**). Moreover, fluorescence seemed more intense at the edges of the incision, and at 200 μm, fluorescence staining was still visible at its border. This penetration mode is compatible with the rupture of the barrier function of the stratum corneum.

4.6. Influence of encapsulation on antifungal effect

The *in vitro* antifungal susceptibility testing was performed following previous guidelines (Borba-Santos et al., 2015; CLSI, 2008). MICs and MFCs of itraconazole-loaded NLC, as well as free itraconazole, fluconazole and amphotericin B standard antifungals for *S. brasiliensis* and *C. albicans* are shown in **Table 3**. Itraconazole-loaded NLC and free itraconazole showed very similar results, indicating that encapsulation does not hinder the antifungal effect of the drug. In addition, we observed that azoles exerted a fungistatic effect, while amphotericin B effect is most likely fungicidal (MFC = 2 μg/mL) as previously described in the literature (Borba-Santos et al., 2015; Yenisehirli et al., 2015).

Having demonstrated that encapsulation does not hinder itraconazole antifungal effect, we proceeded to evaluate the efficacy of the NLC in an invertebrate model of fungal infection by *S. brasiliensis* or *C. albicans* yeasts. The *G. mellonella* larval model was employed, in which pro-leg injection was used as the administration route (**Figure 8A**). We acknowledge that this route better mimics systemic administration and not cutaneous delivery, but it allowed us to assess systemic toxicity and efficacy while following guidelines for reduction, refinement and replacement in animal studies, since this model does not require IACUC approval. The unloaded and itraconazole-loaded NLC showed no toxicity on the larvae, and 100% survival was observed in non-infected larvae **(Figure 8B**).

After 30 minutes of infection, the larvae were treated with 20 mg/Kg or 40 mg/Kg of itraconazole-loaded NLC, and evaluated for morbidity and mortality over the five-day time window. Despite the low virulence presented by *S. brasiliensis* clinical isolate (Sb54 strain), demonstrated by the few individuals killed by the end of the experiment, the nanocarrier increased the larva survival from 80% to 100% (**Figure 8C)**. It was possible to observe only a slight improvement in the health index with the nanocarrier treatment, which might result from the low virulence of the strain and its small effect on the larvae activity, cocoon formation and melanization (**Figure 8D**). As proof of concept of the antifungal efficacy of the nanocarrier against more virulent fungus strain, the effect of NLC treatment was also evaluated in the larvae infected with *C.*

albicans. Larvae infection with this strain led to 70% mortality on the 4th post-infection (**Figure 8E**). Itraconazole loaded-NLC protected ~100% of fungal infection at 20-40 mg/Kg; in contrast, itraconazole dispersion at either dose did not preserve the health status and life of the larvae (**Figure 8E and F**).

As control, the unloaded nanocarrier was also evaluated under the same conditions and neither inhibited fungal growth *in vitro* nor presented antifungal effects in infected *G. mellonella* larvae with S. *brasiliensis* or *C. albicans* yeasts (data not shown), indicating that the formulation did not interfere with the antifungal efficacy assay.

5. Discussion

Itraconazole is considered the standard pharmacological treatment for fungal infections caused by *Sporothrix* spp. despite reported therapeutic failures in feline sporotrichosis, systemic adverse effects, drug-drug interactions and low water solubility and oral bioavailability (Gilaberte et al., 2014; Kumar and Goindi, 2014). Thus, the need for alternative drug delivery platforms that provide localization in cutaneous lesions and improve current treatment strategies justifies the current study (Ishida et al., 2018; Kauffman et al., 2007).

Because the choice of type and concentration of the oil phase and surfactant is very important for the physicochemical characteristics and stability of nanocarriers (Carvalho et al., 2019), we started this study assessing how the ratio among these components affected NLC formation. A more homogenous size distribution, indicative of sample quality improvement, was observed when the ratio solid:liquid lipid increased from 3:7 to 5:5 or 7:3 (w/w), and when the concentration of Tween and Span doubled from 1.5 to 3% each.

Even though increases in the surfactant concentration are often associated with a higher risk of skin irritation (Lopes et al., 2015; Pepe et al., 2013), overall nanocarrier safety was demonstrated in this study using two methods. The NLC irritation potential was investigated using the HET-CAM test to address local (to the skin) safety, and the score lower than 0.9 enabled its classification as

non-irritant. This results is supported by previous reports in which lipid nanocarriers were classified as slightly irritant or non-irritant using the HET-CAM model, a classification further confirmed by other methods (Fangueiro et al., 2016; Wolf et al., 2009). Despite our goal of local NLC administration, systemic toxicity was investigated (in case small amounts were systemically absorbed) by measuring the survival of non-infected *G. melonella* larvae after unloaded NLC pro-leg administration. This is considered an alternative model to animal use, and its advantages include the facts that the larvae are easy to breed, and that the assay does not require specialized facilities or institutional committee for animal use approval (Clavijo-Giraldo et al., 2016). Due to the similarities between the insect immune response and the innate response of mammals, gastrointestinal and hepatic systems, this model has been employed to assess the toxicity of food preservatives, ionic liquids, and delivery systems (Maguire et al., 2016; Migotto et al., 2018). The survival of the non-infected larvae following NLC administration suggests its safety. It is worth noting that other methods support the safety of glyceryl behenate-based nanocarriers, including the Draize patch test and *in vivo* measurement of TEWL (Jain et al., 2019).

Consistent with its use as a matrix for sustained/prolonged release (Graves et al., 2015), glyceryl behenate has a relatively high melting point (T_{peak}= 70 °C), which was reduced upon tricaprylin addition. A similar phenomenon has been previously described in lipid nanocarriers due to the addition of glyceryl caprylate/caprate and phosphatidylcholine, which disturbed the solid lipid crystallinity, resulting in a lower melting point, better drug accommodation in the nanocarrier, and greater encapsulation efficiency (Jansook et al., 2019). Despite this reduction in the melting point, the fact that it is still above biological temperatures indicates that the solid nature of the nanocarrier will be preserved during topical administration. Since drug release from lipid nanoparticles with a solid core is slower than that from liquid core (as in nanoemulsions), it is reasonable to assume that the developed NLC might enable depot formation and prolong itraconazole release in the lesions (Ruktanonchai et al., 2009). Because only the small endothermic peak attributed to itraconazole nematic phase (70-90 °C) was observed in the drug-loaded NLC

DSC chart, a decrease in drug crystallinity due to its incorporation in the lipid nanocarrier is probable. In addition to the lipids, the surfactants employed in the production of the NLC might aid drug solubilization in the system (Fachinetti et al., 2018).

Assessment of penetration using fluorescence microscopy demonstrated a preferential accumulation of the dye along the incision border, which was expected since the main penetration barrier was damaged in this region, and corroborates our penetration studies showing that higher amounts of itraconazole reach deeper skin layers when the tissue was damaged. Although higher compared to the intact skin, transdermal delivery mediated by NLC was lower than that mediated by the solution, and itraconazole encapsulation increased the *skin/receptor phase* ratio at 24 h by ~1.8-fold. This indicates that the NLC improved cutaneous targeting of itraconazole even when the tissue barrier was damaged, which has important implications when it comes to avoiding drug systemic exposure and adverse effects. This targeting effect was not as pronounced as previously observed for adenosine (Ng et al., 2017), which might be justified by the higher lipophilicity of itraconazole (logP>5) and the consequent retention in the skin (especially in non-polar layers) that can be expected independently on the presence of an incision.

Several mechanisms have been postulated to explain cutaneous targeting. One of them is the preferred sequestration of lipid nanoparticles in/around follicular structures (Chen et al., 2006; Lademann et al., 1999; Shamma and Aburahma, 2014), but this mechanism alone cannot explain itraconazole localization in the skin with disrupted barrier. Cutaneous targeting has been linked to the mode of drug association with the particle: association to the particle surface was deemed important, while the sole presence of specific lipids was not sufficient (Schäfer-Korting et al., 2007; Sivaramakrishnan et al., 2004). It was postulated that the rapid release in these circumstances might induce epidermal targeting (Schäfer-Korting et al., 2007). Additionally, Hung *et al*. reported association between NLC and keratinocytes, due to both internalization and membrane adsorption (Hung et al., 2015). Although internalization by specialized mechanisms cannot be expected in the

skin employed here (due to the low/no viability of frozen tissues), nanocarrier adsorption at the cell membrane can help to justify skin targeting.

Even though the NLC can be applied as obtained (it is approximately 5-fold more viscous than a regular aqueous solution) if the lesion is covered, prior studies have incorporated NLCs in hydrogels of carbopol and hydroxyl ethylcellulose, among other polymers, to improve residence time (El-Sheridy et al., 2019). We have not investigated the effect of gelling agents on itraconazole release and tissue penetration, but it is possible to speculate about the outcomes based on the literature. Yu *et al*. observed that incorporation of quercetin-loaded NLC in gels reduced cumulative drug release in ~8% compared to the NLC aqueous dispersion due to the additional diffusional barrier imposed by the three-dimensional network structure of the gel (Yu et al., 2018). Ravani *et al*. (Ravani et al., 2013) reported that hydrogels limited the diffusion of clotrimazol (loaded in NLC) through the vaginal mucosa, serving as a suitable delivery system for vaginal fungal infections. Additionally, incorporation of lipid nanoparticles in gels has been reported to increase cutaneous delivery of drugs (Bagde et al., 2019; El-Sheridy et al., 2019). Based on these reports, increased tissue delivery might be expected should the NLC be incorporated in hydrogels.

To date, there are no topical formulations commercially available for itraconazole. Few studies have proposed topical and/or transdermal itraconazole delivery for treatment of basal skin carcinoma (Carbone et al., 2018) and infections caused by *Candida*, *Aspergillus*, and *Cryptococcus* (Chudasama et al., 2011; El-Sheridy et al., 2019; Nesseem, 2001), but to the best of our knowledge, one focused on topical itraconazole delivery (using microemulsions) for sporotrichosis treatment (Ferreira et al., 2020). Although the investigated nanocarriers differed in composition, physicochemical properties and itraconazole dose from ours (all of them representing factors capable of affecting cutaneous bioavailability) (Carvalho et al., 2017a; Carvalho et al., 2017b; Pepe et al., 2016), it is possible to establish comparisons. Using lipid nanocarriers in a gel containing paclitaxel at a lower dose (0.05% w/w), El-Sheridy *et al.* reported that 59-66% of itraconazole topically applied dose penetrated the skin after 6 h, and 1% reached the receptor phase (El-Sheridy

et al., 2019). Our NLC delivered a lower percentage of the dose to the skin and across the tissue (even in damaged skin), which was consistent with our goal of providing a localized and prolonged topical release. On the other hand, Chudassama *et al*. (Chudasama et al., 2011) reported that over 80% of the itraconazole dose was delivered across rodent skin (which is regarded as more permeable than porcine or human skin) using a microemulsion gel. Considering that 1% of itraconazole was reportedly incorporated in the microemulsion gel, these results imply that large amounts of drug are delivered across the skin. Ferreira *et al.* developed microemulsions for the co-delivery of itraconazole and clotrimazole, and an interesting synergistic effect on itraconazole penetration was observed upon its co-incorporation with clotrimazole, suggesting the ability of the later to serve as a penetration enhancer (Ferreira et al., 2020).

Another interesting property of the NLC developed here was its ability to decrease TEWL, which might aid lesion hydration maintenance. NLC-mediated reduction on TEWL and improvement of hydration is not a new concept, having been previously reported in intact skin and attributed to the ability of the particles to form a film, become absorbed in the intercellular space of the SC and reestablish the skin's barrier function (Loo et al., 2013). Our results built upon these observations and demonstrated reduction of TEWL when the skin was subjected to damage. Considering that hydration is essential for faster healing, reduction of scarring, and maintenance of growth factors at the healing site, the NLC structure *per se* might contribute to the healing process (Ousey et al., 2016). This remains to be investigated.

Finally, the *in vitro* antifungal assay confirmed that encapsulation did not hinder the antifungal effect against *S. brasiliensis* and *C. albicans* yeasts, which corroborate previous studies (Spadari et al., 2019). To further demonstrate itraconazole activity when loaded in the nanocarrier, we employed the *G. mellonella* model, which is widely used for toxicity and antifungal susceptibility investigations. Although this method was employed for other nanomaterials, it had not been previously used for evaluation of antifungal efficacy of NLCs. To illustrate, a previous study demonstrated the success of the model in the evaluation of antifungal activity of Ag-

nanoparticles in an *Aspergillus fumigatus* model, and of polysaccharide-based nanoparticles in larvae infected with *C. albicans*, *Cryptococcus neoformans* and *Cryptococcus gattii* (Siemer et al., 2019; Spadari et al., 2019). Our results demonstrated that, in spite of the low virulence of the *S. brasiliensis* yeasts, the itraconazole-loaded NLC improved larval survival to approximately 100%. One possible reason for the low virulence observed in the study is the time-course employed; Clavijo-Giralo et al. have observed higher larvae mortality over the course of 15 days (Clavijo-Giraldo et al., 2016). Other studies also reported virulence attenuation in the *G. mellonella* model (Lozoya-Perez et al., 2019). As proof of concept, the antifungal efficacy was confirmed using a virulent strain of *C. albicans*, wherein the itraconazole-loaded NLC treatment significantly reduced the larval morbidity and mortality. Thus, itraconazole incorporation in the NLC does not hinder its pharmacological effects. Additionally, the NLC was more efficacious than the itraconazole dispersion in PBS, which may be attributed to the low aqueous solubility of itraconazole. During dilution of the DMSO stock solution, signs of drug precipitation (represented mainly by areas of cloudiness in the system) could be observed, suggesting that a lower drug concentration in the dissolved form was available *in vivo*. Therefore, it is reasonable to suggest that itraconazole precipitation compromised its antifungal effect, as previously described for other azole antifungals such as ketoconazole (Ruff et al., 2017). These results also support the ability of the NCLs to prevent itraconazole precipitation, enabling its therapeutic efficacy. Future studies will assess the effect of the NLC on *S. brasiliensis* virulent strains in order to further clarify its effect on the morbidity and mortality of *G. mellonella* larvae and in a murine model of fungal infection.

6. Conclusion

Our results demonstrate the possibility of obtaining itraconazole-loaded nanostructured lipid carriers within the nanometric range and the ability of the nanoparticles to preserve skin hydration even in damaged tissues and to improve cutaneous targeting of the drug. Importantly, nanoencapsulation did not hinder the antifungal effects of the drug against *S. brasiliensis* and *C.*

albicans. With this study, we aim to contribute to the development of an advantageous and effective strategy for localized treatment of sporotrichosis lesions.

Acknowledgments

The authors thank Prof. Dr. Anderson Messias Rodrigues from Federal University of São Paulo (São Paulo/SP, Brazil) for kindly providing the *Sporothrix brasiliensis* Sb54 strain. This study was supported by São Paulo Research Foundation (FAPESP, 2013/16617-7, 2018/13877-1, 2015/07993-0, 2017/19374-9), National Council for Scientific and Technological Development (CNPq/PIBIT and PIBIC), CAPES (finance code 001) and INCT-NANOFARMA (FAPESP #2014/50928-2, CNPq# 465687/2014-8). Confocal microscopy was conducted at the CEFAP core facility (Institute of Biomedical Sciences, University of São Paulo).

References

Almeida-Paes, R., de Oliveira, M.M.E., Freitas, D.F.S., do Valle, A.C.F., Zancopé-Oliveira, R.M., Gutierrez-Galhardo, M.C., 2014. Sporotrichosis in Rio de Janeiro, Brazil: Sporothrix brasiliensis is associated with atypical clinical presentations. PLoS Negl Trop Dis 8, e3094-e3094.

Alzuguir, C.L.C., Pereira, S.A., Magalhães, M.A.F.M., Almeida-Paes, R., Freitas, D.F.S., Oliveira, L.F.A., Pimentel, M.I.F., 2020. Geo-epidemiology and socioeconomic aspects of human sporotrichosis in the municipality of Duque de Caxias, Rio de Janeiro, Brazil, between 2007 and 2016. Transactions of the Royal Society of Tropical Medicine and Hygiene 114, 99-106.

Bagde, A., Patel, K., Kutlehria, S., Chowdhury, N., Singh, M., 2019. Formulation of topical ibuprofen solid lipid nanoparticle (SLN) gel using hot melt extrusion technique (HME) and determining its anti-inflammatory strength. Drug delivery and translational research 9, 816-827.

Borba-Santos, L.P., Rodrigues, A.M., Gagini, T.B., Fernandes, G.F., Castro, R., de Camargo, Z.P., Nucci, M., Lopes-Bezerra, L.M., Ishida, K., Rozental, S., 2015. Susceptibility of Sporothrix brasiliensis isolates to amphotericin B, azoles, and terbinafine. Medical mycology 53, 178-188.

Bose, S., Du, Y., Takhistov, P., Michniak-Kohn, B., 2013. Formulation optimization and topical delivery of quercetin from solid lipid based nanosystems. International Journal of Pharmaceutics 441, 56-66.

Carbone, C., Martins-Gomes, C., Pepe, V., Silva, A.M., Musumeci, T., Puglisi, G., Furneri, P.M., Souto, E.B., 2018. Repurposing itraconazole to the benefit of skin cancer treatment: A combined azole-DDAB nanoencapsulation strategy. Colloids and surfaces. B, Biointerfaces 167, 337-344.

Carvalho, V.F., de Lemos, D.P., Vieira, C.S., Migotto, A., Lopes, L.B., 2017a. Potential of Non-aqueous Microemulsions to Improve the Delivery of Lipophilic Drugs to the Skin. AAPS PharmSciTech 18, 1739-1749.

Carvalho, V.F.M., Migotto, A., Giacone, D.V., de Lemos, D.P., Zanoni, T.B., Maria-Engler, S.S., Costa-Lotufo, L.V., Lopes, L.B., 2017b. Co-encapsulation of paclitaxel and C6 ceramide in tributyrin-containing nanocarriers improve co-localization in the skin and potentiate cytotoxic effects in 2D and 3D models. Eur J Pharm Sci 109, 131-143.

Carvalho, V.F.M., Salata, G.C., de Matos, J.K.R., Costa-Fernandez, S., Chorilli, M., Steiner, A.A., de Araujo, G.L.B., Silveira, E.R., Costa-Lotufo, L.V., Lopes, L.B., 2019. Optimization of composition and obtainment parameters of biocompatible nanoemulsions intended for intraductal administration of piplartine (piperlongumine) and mammary tissue targeting. Int J Pharm 567, 118460.

Champion, O.L., Titball, R.W., Bates, S., 2018. Standardization of G. mellonella Larvae to Provide Reliable and Reproducible Results in the Study of Fungal Pathogens. J Fungi (Basel) 4, 108.

Chen, H., Chang, X., Du, D., Liu, W., Liu, J., Weng, T., Yang, Y., Xu, H., Yang, X., 2006. Podophyllotoxin-loaded solid lipid nanoparticles for epidermal targeting. Journal of controlled release : official journal of the Controlled Release Society 110, 296-306.

Chen, J., Wei, N., Lopez-Garcia, M., Ambrose, D., Lee, J., Annelin, C., Peterson, T., 2017. Development and evaluation of resveratrol, Vitamin E, and epigallocatechin gallate loaded lipid nanoparticles for skin care applications. Eur J Pharm Biopharm 117, 286-291.

Chudasama, A., Patel, V., Nivsarkar, M., Vasu, K., Shishoo, C., 2011. Investigation of microemulsion system for transdermal delivery of itraconazole. Journal of advanced pharmaceutical technology & research 2, 30-38.

Cirri, M., Maestrini, L., Maestrelli, F., Mennini, N., Mura, P., Ghelardini, C., Di Cesare Mannelli, L., 2018. Design, characterization and in vivo evaluation of nanostructured lipid carriers (NLC) as a new drug delivery system for hydrochlorothiazide oral administration in pediatric therapy. Drug delivery 25, 1910-1921.

Clavijo-Giraldo, D.M., Matinez-Alvarez, J.A., Lopes-Bezerra, L.M., Ponce-Noyola, P., Franco, B., Almeida, R.S., Mora-Montes, H.M., 2016. Analysis of Sporothrix schenckii sensu stricto and Sporothrix brasiliensis virulence in Galleria mellonella. Journal of microbiological methods 122, 73-77.

CLSI, 2008. Reference Method for Broth dilution antifungal susceptibility testing of yeasts. Approved standard M27-A3, Clinical and Laboratory Standards Institute, USA.

Contri, R.V., Fiel, L.A., Alnasif, N., Pohlmann, A.R., Guterres, S.S., Schafer-Korting, M., 2016. Skin penetration and dermal tolerability of acrylic nanocapsules: Influence of the surface charge and a chitosan gel used as vehicle. Int J Pharm 507, 12-20.

Danaei, M., Dehghankhold, M., Ataei, S., Hasanzadeh Davarani, F., Javanmard, R., Dokhani, A., Khorasani, S., Mozafari, M.R., 2018. Impact of Particle Size and Polydispersity Index on the Clinical Applications of Lipidic Nanocarrier Systems. Pharmaceutics 10.

Das, S., Ng, W.K., Tan, R.B.H., 2012. Are nanostructured lipid carriers (NLCs) better than solid lipid nanoparticles (SLNs): development, characterizations and comparative evaluations of clotrimazole-loaded SLNs and NLCs? European journal of pharmaceutical sciences : official journal of the European Federation for Pharmaceutical Sciences 47, 139-151.

El-Sheridy, N.A., Ramadan, A.A., Eid, A.A., El-Khordagui, L.K., 2019. Itraconazole lipid nanocapsules gel for dermatological applications: In vitro characteristics and treatment of induced cutaneous candidiasis. Colloids Surf B Biointerfaces 181, 623-631.

Espinel-Ingroff, A., Chaturvedi, V., Fothergill, A., Rinaldi, M.G., 2002. Optimal testing conditions for determining MICs and minimum fungicidal concentrations of new and established antifungal agents for uncommon molds: NCCLS collaborative study. J Clin Microbiol 40, 3776-3781.

Fachinetti, N., Rigon, R.B., Eloy, J.O., Sato, M.R., Dos Santos, K.C., Chorilli, M., 2018. Comparative Study of Glyceryl Behenate or Polyoxyethylene 40 Stearate-Based Lipid Carriers for Trans-Resveratrol Delivery: Development, Characterization and Evaluation of the In Vitro Tyrosinase Inhibition. AAPS PharmSciTech 19, 1401-1409.

Fangueiro, J.F., Calpena, A.C., Clares, B., Andreani, T., Egea, M.A., Veiga, F.J., Garcia, M.L., Silva, A.M., Souto, E.B., 2016. Biopharmaceutical evaluation of epigallocatechin gallate-loaded cationic lipid nanoparticles (EGCG-LNs): In vivo, in vitro and ex vivo studies. Int J Pharm 502, 161-169.

Ferreira, P.G., Noronha, L., Teixeira, R., Vieira, I., Borba-Santos, L.P., Viçosa, A., de Moraes, M., Calil-Elias, S., de Freitas, Z., da Silva, F.C., Rozental, S., Futuro, D.O., Ferreira, V.F., 2020. Investigation of a Microemulsion Containing Clotrimazole and Itraconazole for Transdermal Delivery for the Treatment of Sporotrichosis. Journal of pharmaceutical sciences 109, 1026-1034.

Frenkel, M., Mandelblat, M., Alastruey-Izquierdo, A., Mendlovic, S., Semis, R., Segal, E., 2016. Pathogenicity of Candida albicans isolates from bloodstream and mucosal candidiasis assessed in mice and Galleria mellonella. J Mycol Med 26, 1-8.

Friedman, D.Z.P., Schwartz, I.S., 2019. Emerging Fungal Infections: New Patients, New Patterns, and New Pathogens. J Fungi (Basel) 5, 67.

Gilaberte, Y., Aspiroz, C., Alejandre, M.C., Andres-Ciriano, E., Fortuño, B., Charlez, L., Revillo, M.J., Hamblin, M.R., Rezusta, A., 2014. Cutaneous sporotrichosis treated with photodynamic therapy: an in vitro and in vivo study. Photomed Laser Surg 32, 54-57.

Graves, R.A., Ledet, G.A., Nation, C.A., Pramar, Y.V., Bostanian, L.A., Mandal, T.K., 2015. Effect of squalane on mebendazole-loaded Compritol® nanoparticles. J Biomater Sci Polym Ed 26, 868-880.

Gremião, I.D.F., Miranda, L.H.M., Reis, E.G., Rodrigues, A.M., Pereira, S.A., 2017. Zoonotic Epidemic of Sporotrichosis: Cat to Human Transmission. PLoS Pathog 13, e1006077-e1006077.

Gupta, S., Bansal, R., Gupta, S., Jindal, N., Jindal, A., 2013. Nanocarriers and nanoparticles for skin care and dermatological treatments. Indian Dermatol Online J 4, 267-272.

Hung, C.-F., Chen, W.-Y., Hsu, C.-Y., Aljuffali, I.A., Shih, H.-C., Fang, J.-Y., 2015. Cutaneous penetration of soft nanoparticles via photodamaged skin: Lipid-based and polymer-based nanocarriers for drug delivery. European journal of pharmaceutics and biopharmaceutics : official journal of Arbeitsgemeinschaft fur Pharmazeutische Verfahrenstechnik e.V 94, 94-105.

Ishida, K., Castro, R.A., Torrado, J.J., Serrano, D.R., Borba-Santos, L.P., Quintella, L.P., de Souza, W., Rozental, S., Lopes-Bezerra, L.M., 2018. Efficacy of a poly-aggregated formulation of amphotericin B in treating systemic sporotrichosis caused by Sporothrix brasiliensis. Medical mycology 56, 288-296.

Jain, A., Hurkat, P., Jain, S.K., 2019. Development of liposomes using formulation by design: Basics to recent advances. Chem Phys Lipids.

Jansook, P., Fülöp, Z., Ritthidej, G.C., 2019. Amphotericin B loaded solid lipid nanoparticles (SLNs) and nanostructured lipid carrier (NLCs): physicochemical and solid-solution state characterizations. Drug development and industrial pharmacy 45, 560-567.

Kauffman, C.A., Bustamante, B., Chapman, S.W., Pappas, P.G., Infectious Diseases Society of, A., 2007. Clinical practice guidelines for the management of sporotrichosis: 2007 update by the Infectious Diseases Society of America. Clin Infect Dis 45, 1255-1265.

Kumar, N., Goindi, S., 2014. Statistically designed nonionic surfactant vesicles for dermal delivery of itraconazole: characterization and in vivo evaluation using a standardized Tinea pedis infection model. International journal of pharmaceutics 472, 224-240.

Lademann, J., Weigmann, H., Rickmeyer, C., Barthelmes, H., Schaefer, H., Mueller, G., Sterry, W., 1999. Penetration of titanium dioxide microparticles in a sunscreen formulation into the horny layer and the follicular orifice. Skin Pharmacol Appl Skin Physiol 12, 247-256.

Loo, C., Basri, M., Ismail, R., Lau, H., Tejo, B., Kanthimathi, M., Hassan, H., Choo, Y., 2013. Effect of compositions in nanostructured lipid carriers (NLC) on skin hydration and occlusion. Int J Nanomedicine 8, 13-22.

Lopes, L.B., Garcia, M.T., Bentley, M.V., 2015. Chemical penetration enhancers. Therapeutic delivery 6, 1053-1061.

Lozoya-Perez, N.E., Casas-Flores, S., de Almeida, J.R.F., Martinez-Alvarez, J.A., Lopez-Ramirez, L.A., Jannuzzi, G.P., Trujillo-Esquivel, E., Estrada-Mata, E., Almeida, S.R., Franco, B., Lopes-Bezerra, L.M., Mora-Montes, H.M., 2019. Silencing of OCH1 unveils the role of Sporothrix schenckii N-linked glycans during the host-fungus interaction. Infection and drug resistance 12, 67-85.

Maguire, R., Duggan, O., Kavanagh, K., 2016. Evaluation of Galleria mellonella larvae as an in vivo model for assessing the relative toxicity of food preservative agents. Cell Biol Toxicol 32, 209-216.

McKenzie, B., Kay, G., Matthews, K.H., Knott, R.M., Cairns, D., 2015. The hen's egg chorioallantoic membrane (HET-CAM) test to predict the ophthalmic irritation potential of a cysteamine-containing gel: Quantification using Photoshop(R) and ImageJ. Int J Pharm 490, 1-8.

Migotto, A., Carvalho, V.F.M., Salata, G.C., da Silva, F.W.M., Yan, C.Y.I., Ishida, K., Costa-Lotufo, L.V., Steiner, A.A., Lopes, L.B., 2018. Multifunctional nanoemulsions for intraductal delivery as a new platform for local treatment of breast cancer. Drug Deliv 25, 654-667.

Miller, D.A., DiNunzio, J.C., Yang, W., McGinity, J.W., Williams, R.O., 3rd, 2008. Targeted intestinal delivery of supersaturated itraconazole for improved oral absorption. Pharm Res 25, 1450-1459.

Mojeiko, G., de Brito, M., Salata, G.C., Lopes, L.B., 2019. Combination of microneedles and microemulsions to increase celecoxib topical delivery for potential application in chemoprevention of breast cancer. Int J Pharm 560, 365-376.

Nesseem, D.I., 2001. Formulation and evaluation of itraconazole via liquid crystal for topical delivery system. J Pharm Biomed Anal 26, 387-399.

Ng, W.Y., Migotto, A., Ferreira, T.S., Lopes, L.B., 2017. Monoolein-alginate beads as a platform to promote adenosine cutaneous localization and wound healing. International journal of biological macromolecules 102, 1104-1111.

Ousey, K., Cutting, K.F., Rogers, A.A., Rippon, M.G., 2016. The importance of hydration in wound healing: reinvigorating the clinical perspective. Journal of wound care 25, 122, 124-130.

Pardeike, J., Hommoss, A., Muller, R.H., 2009. Lipid nanoparticles (SLN, NLC) in cosmetic and pharmaceutical dermal products. Int J Pharm 366, 170-184.

Pardeike, J., Weber, S., Zarfl, H.P., Pagitz, M., Zimmer, A., 2016. Itraconazole-loaded nanostructured lipid carriers (NLC) for pulmonary treatment of aspergillosis in falcons. European journal of pharmaceutics and biopharmaceutics : official journal of Arbeitsgemeinschaft fur Pharmazeutische Verfahrenstechnik e.V 108, 269-276.

Parmentier, J., Tan, E.H., Low, A., Möschwitzer, J.P., 2017. Downstream drug product processing of itraconazole nanosuspension: Factors influencing drug particle size and dissolution from nanosuspension-layered beads. International Journal of Pharmaceutics 524, 443-453.

Pepe, D., Carvalho, V.F., McCall, M., de Lemos, D.P., Lopes, L.B., 2016. Transportan in nanocarriers improves skin localization and antitumor activity of paclitaxel. Int J Nanomedicine 11, 2009-2019.

Pepe, D., McCall, M., Zheng, H., Lopes, L.B., 2013. Protein transduction domain-containing microemulsions as cutaneous delivery systems for an anticancer agent. J Pharm Sci 102, 1476-1487.

Pinto Reis, C., Vasques Roque, L., Baptista, M., Rijo, P., 2016. Innovative formulation of nystatin particulate systems in toothpaste for candidiasis treatment. Pharmaceutical development and technology 21, 282-287.

Quinney, S.K., Galinsky, R.E., Jiyamapa-Serna, V.A., Chen, Y., Hamman, M.A., Hall, S.D., Kimura, R.E., 2008. Hydroxyitraconazole, formed during intestinal first-pass metabolism of itraconazole, controls the time course of hepatic CYP3A inhibition and the bioavailability of itraconazole in rats. Drug metabolism and disposition: the biological fate of chemicals 36, 1097-1101.

Ravani, L., Esposito, E., Bories, C., Moal, V.L.-L., Loiseau, P.M., Djabourov, M., Cortesi, R., Bouchemal, K., 2013. Clotrimazole-loaded nanostructured lipid carrier hydrogels: thermal analysis and in vitro studies. International journal of pharmaceutics 454, 695-702.

Ruff, A., Fiolka, T., Kostewicz, E.S., 2017. Prediction of Ketoconazole absorption using an updated in vitro transfer model coupled to physiologically based pharmacokinetic modelling. European journal of pharmaceutical sciences : official journal of the European Federation for Pharmaceutical Sciences 100, 42-55.

Ruktanonchai, U., Bejrapha, P., Sakulkhu, U., Opanasopit, P., Bunyapraphatsara, N., Junyaprasert, V., Puttipipatkhachorn, S., 2009. Physicochemical characteristics, cytotoxicity, and antioxidant activity of three lipid nanoparticulate formulations of alpha-lipoic acid. AAPS PharmSciTech 10, 227-234.

Schäfer-Korting, M., Mehnert, W., Korting, H.-C., 2007. Lipid nanoparticles for improved topical application of drugs for skin diseases. Advanced drug delivery reviews 59, 427-443.

Shamma, R.N., Aburahma, M.H., 2014. Follicular delivery of spironolactone via nanostructured lipid carriers for management of alopecia. International journal of nanomedicine 9, 5449-5460.

Siemer, S., Westmeier, D., Vallet, C., Becker, S., Voskuhl, J., Ding, G.-B., Thines, E., Stauber, R.H., Knauer, S.K., 2019. Resistance to Nano-Based Antifungals Is Mediated by Biomolecule Coronas. ACS Appl Mater Interfaces 11, 104-114.

Silva, M.B.T.d., Costa, M.M.d.M., Torres, C.C.d.S., Galhardo, M.C.G., Valle, A.C.F.d., Magalhães, M.d.A.F.M., Sabroza, P.C., Oliveira, R.M.d., 2012. Urban sporotrichosis: a neglected epidemic in Rio de Janeiro, Brazil. Cadernos de saude publica 28, 1867-1880.

Sivaramakrishnan, R., Nakamura, C., Mehnert, W., Korting, H.C., Kramer, K.D., Schäfer-Korting, M., 2004. Glucocorticoid entrapment into lipid carriers--characterisation by parelectric spectroscopy and influence on dermal uptake. Journal of controlled release : official journal of the Controlled Release Society 97, 493-502.

Six, K., Berghmans, H., Leuner, C., Dressman, J., Van Werde, K., Mullens, J., Benoist, L., Thimon, M., Meublat, L., Verreck, G., Peeters, J., Brewster, M., Van den Mooter, G., 2003. Characterization of solid dispersions of itraconazole and hydroxypropylmethylcellulose prepared by melt extrusion, Part II. Pharm Res 20, 1047-1054.

Souto, E.B., Muller, R.H., 2008. Cosmetic features and applications of lipid nanoparticles (SLN, NLC). Int J Cosmet Sci 30, 157-165.

Spadari, C.C., de Bastiani, F., Lopes, L.B., Ishida, K., 2019. Alginate nanoparticles as non-toxic delivery system for miltefosine in the treatment of candidiasis and cryptococcosis. Int J Nanomedicine 14, 5187-5199.

Srivatsan, V., Dasgupta, A.K., Kale, P., Datla, R.R., Soni, D., Patel, M., Patel, R., Mavadhiya, C., 2004. Simultaneous determination of itraconazole and hydroxyitraconazole in human plasma by high-performance liquid chromatography. J Chromatogr A 1031, 307-313.

Vanden Bossche, H., Koymans, L., Moereels, H., 1995. P450 inhibitors of use in medical treatment: focus on mechanisms of action. Pharmacology & therapeutics 67, 79-100.

Wolf, N.B., Küchler, S., Radowski, M.R., Blaschke, T., Kramer, K.D., Weindl, G., Kleuser, B., Haag, R., Schäfer-Korting, M., 2009. Influences of opioids and nanoparticles on in vitro wound healing models. European Journal of Pharmaceutics and Biopharmaceutics 73, 34-42.

Yenisehirli, G., Bulut, N., Yenisehirli, A., Bulut, Y., 2015. In Vitro Susceptibilities of Candida albicans Isolates to Antifungal Agents in Tokat, Turkey. Jundishapur J Microbiol 8, e28057-e28057.

Yu, Y., Feng, R., Yu, S., Li, J., Wang, Y., Song, Y., Yang, X., Pan, W., Li, S., 2018. Nanostructured lipid carrier-based pH and temperature dual-responsive hydrogel composed of carboxymethyl chitosan and poloxamer for drug delivery. International journal of biological macromolecules 114, 462-469.

Figure captions

Figure 1. Variation of size, pdi and zeta potential for 90 days of nanocarriers composed of glycerylbehenate:tricaprylin at 5:5 (w/w) containing 3% tween 80 and 3% span 80. Data shown as average ± standard deviation of 3 formulation batches.

Figure 2. Characterization of itraconazole-loaded NLC. A: Variations of size and pdi of NLC as a function of itraconazole content. B: scanning electron microscopy image, C: transmission electron

microscopy image. Scale bar = 500nm Data shown as average ± standard deviation of 3 formulation batches.

Figure 3. Thermal behavior of selected samples. A-D TG curves of itraconazole (A), glyceryl behenate (B), unloaded lyophilized NLC (C), and lyophilized NLC with 1% itraconazole (D). TG analysis was conducted with 5 mg of samples in platinum pans at heating rate of 10 °C/min, without isotherm, under nitrogen atmosphere (100 mL/min). E-H: DSC curves of itraconazole (A), glyceryl behenate (B), unloaded lyophilized NLC (C), and lyophilized NLC with 1% itraconazole (D). DSC analysis was performed with samples of 2 mg in partially closed aluminum pans at heating rate of 10°C/min, with 3 min isotherm at 25°C, under nitrogen atmosphere (100 mL/min).

Figure 4. Nanocarrier irritation potential. Signs of vascular toxicity (coagulation, lysis and hemorrhage) on the chorioallantoic membrane after 5 minutes of exposure to saline (negative control), NaOH (positive control), unloaded nanocarrier and 1% itraconazole-loaded nanocarrier; representative images. Data shown as average ± standard deviation of 3-5 eggs.

Figure 5. Influence of nanocarrier administration on cutaneous transepidermal water loss (TEWL). A: histological image of the skin subjected to a linear incision (Scale bar = 200 μm); B: Δ transepidermal water loss, calculated as the difference between TEWL values before and after treatment. Data shown as average ± standard deviation of 3-5 replicates in 2 independent experiments. **$p < 0.01$ compared to control (C, water).

Figure 6. Skin penetration of itraconazole as a function of time into the stratum corneum (SC, A), remaining layers of epidermis and dermis (ED, B) and receptor phase (RP, C, index of transdermal delivery). Data represents average ± standard deviation of 4-6 replicates in 2-3 independent experiments. * $p < 0.05$ and ** $p < 0.01$ compared to control on the same type of tissue (intact or incised) at the same time point; [a] $p < 0.05$ or $p < 0.01$ compared to the intact tissue at the same time point.

Figure 7. Evaluation of the depth of rhodamine penetration studied by confocal microscopy. Images in the first two panels were obtained above the skin surface; the white dotted line depicts the border of the incision.

Figure 8. *In vivo* antifungal activity in *Galleria mellonella* larvae infected with yeast form of *Sporothrix brasiliensis* (Sb 54) or *Candida albicans* (SC5314) and treated with itraconazole dispersion in PBS or itraconazol-loaded NLC, both at 20 or 40 mg/kg. A: Illustrative picture of proleg injection in the *G. mellonella* larvae, B: survival rate of non-infected larvae to assess safety of the nanocarrier; C: survival rate of larvae infected with *S. brasiliensis* and treated with itraconazole dispersion in PBS or itraconazol-loaded NLC. D: health index of larvae infected with *S. brasiliensis* and treated with itraconazole in suspension in PBS or itraconazol-loaded NLC; E: survival curves of larvae infected with *C. albicans* and treated with itraconazole in suspension in PBS or itraconazol loaded-NLC; F: health index of larvae infected with *C. albicans* and treated with itraconazole dispersion in PBS or itraconazol loaded-NLC. Data represents average ± standard deviation using 20 larvae for each group. * $p < 0.05$ compared with larvae infected with *S. brasiliensis*, # $p < 0.05$ compared with the with larvae infected with *C. albicans*.

Figure 1

Click here to download high resolution image

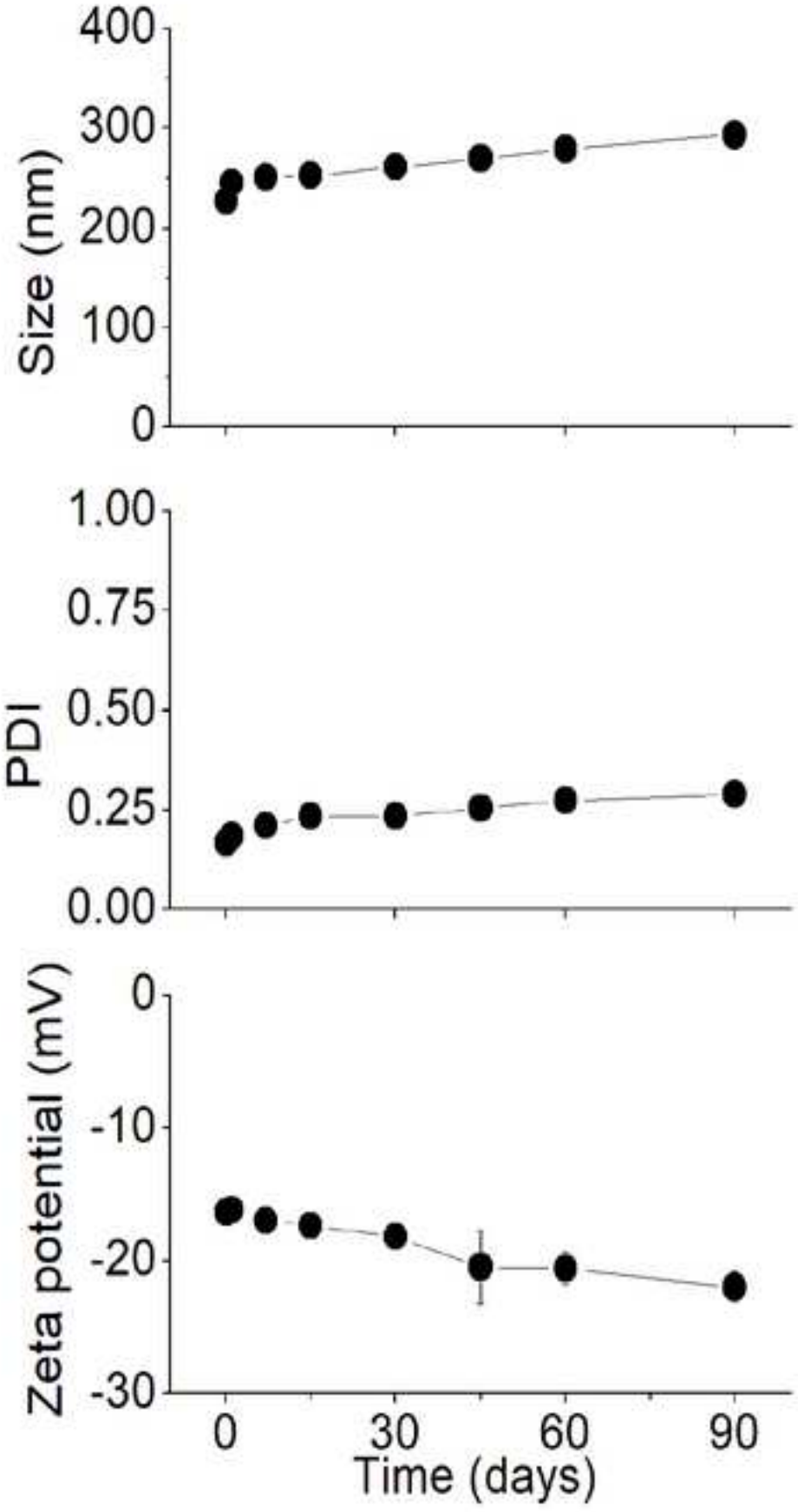

Figure 2

Click here to download high resolution image

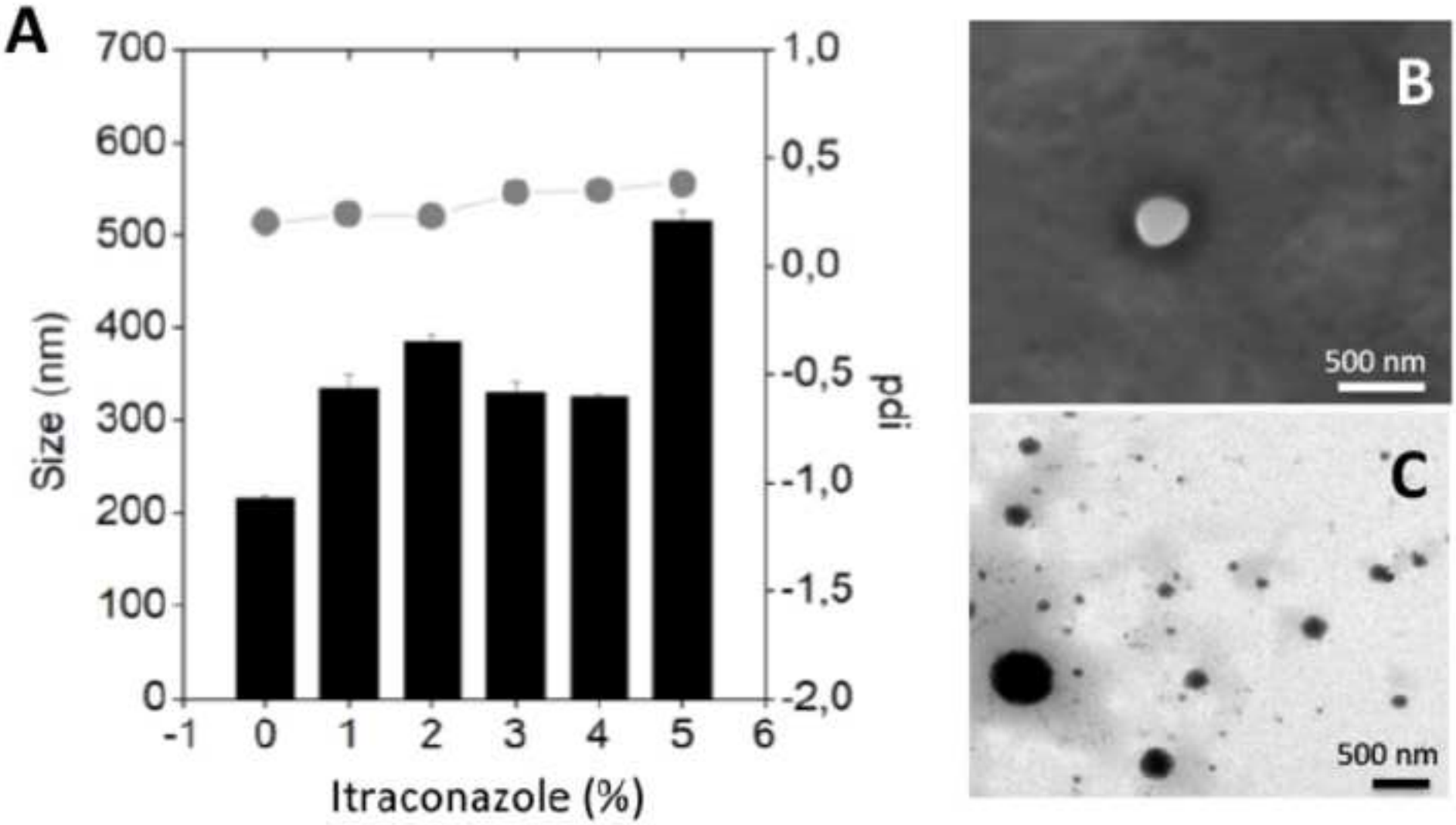

Figure 3

Click here to download high resolution image

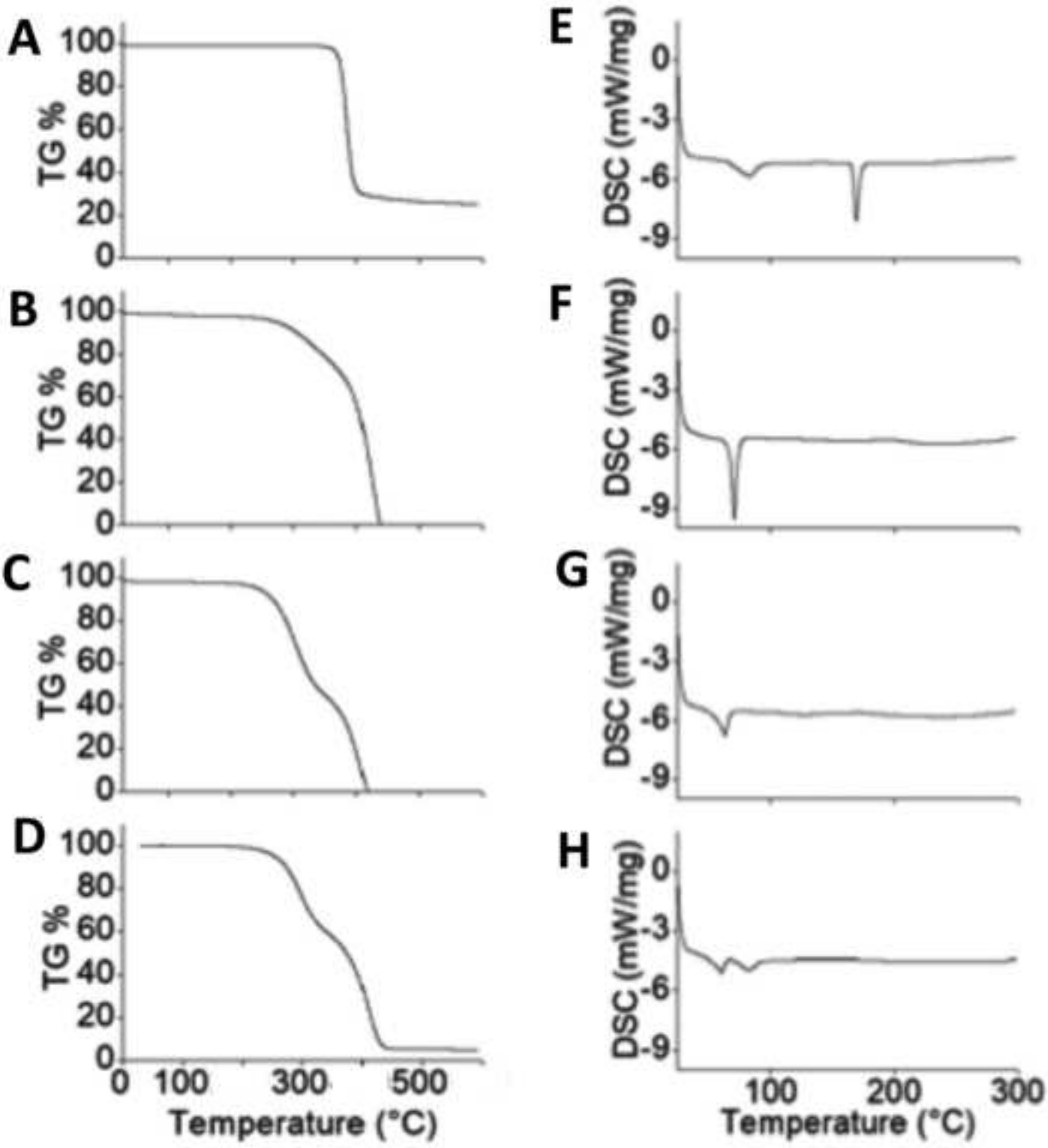

Figure 4

Click here to download high resolution image

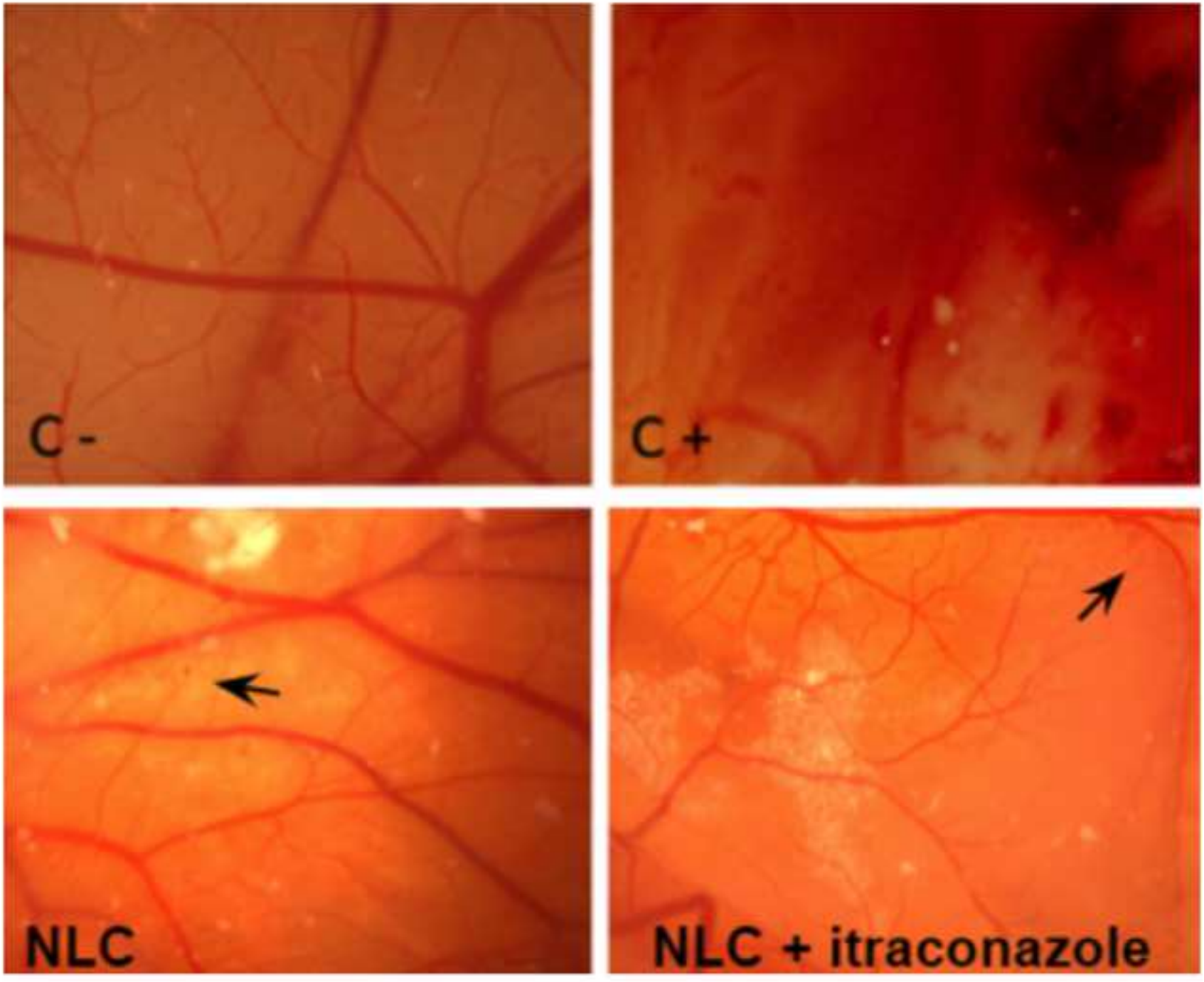

Figure 5

Click here to download high resolution image

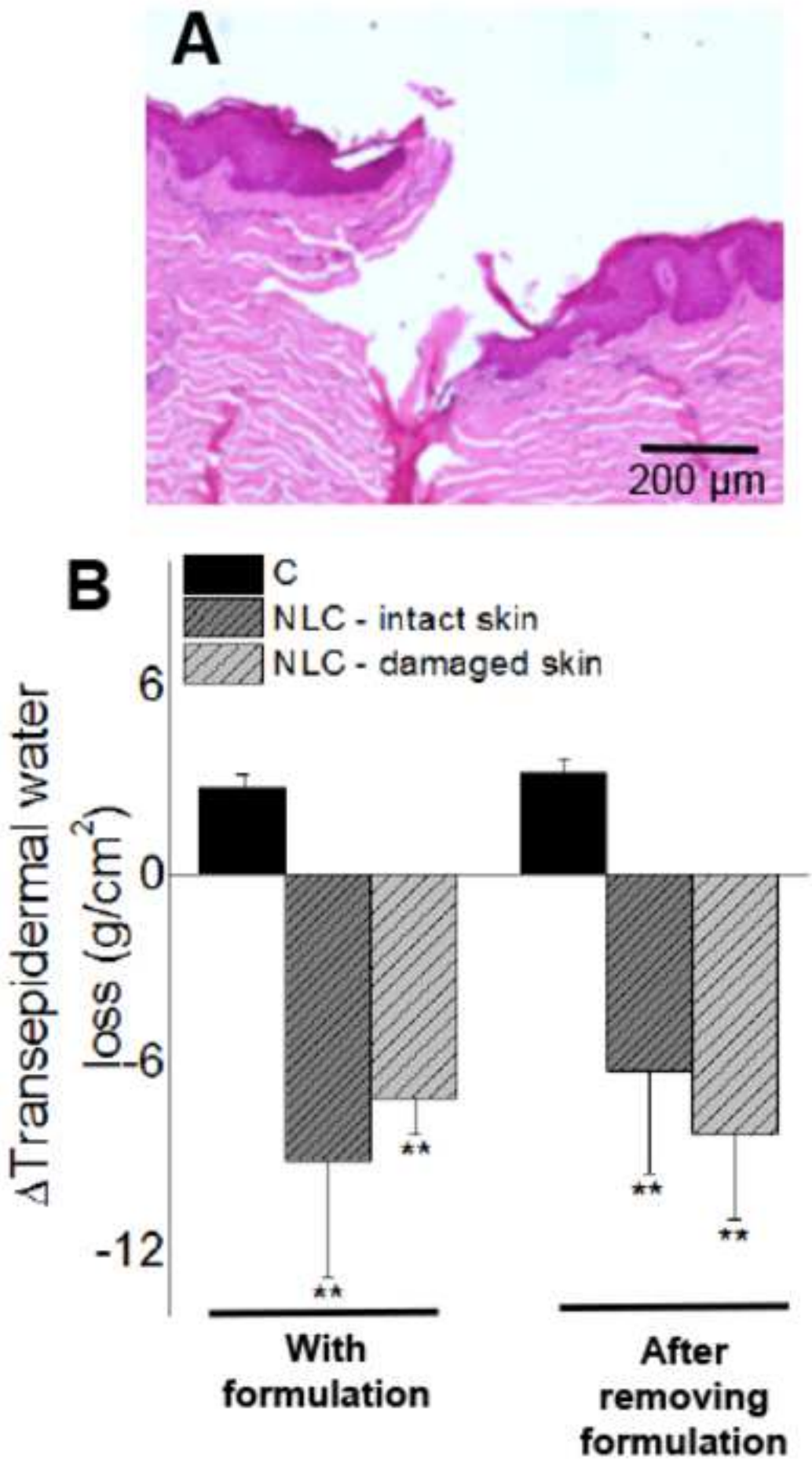

Figure 6

Click here to download high resolution image

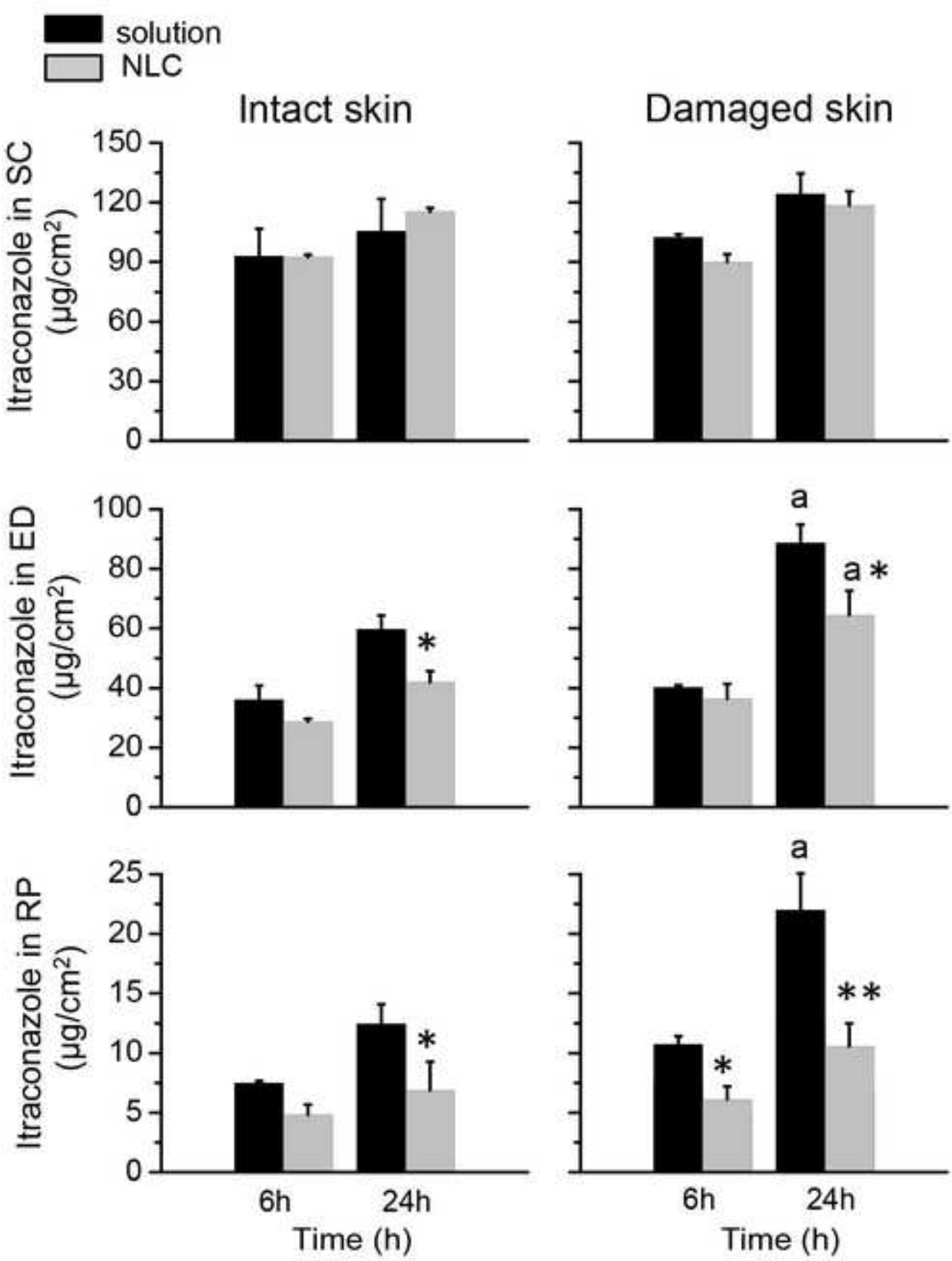

Figure 7

Click here to download high resolution image

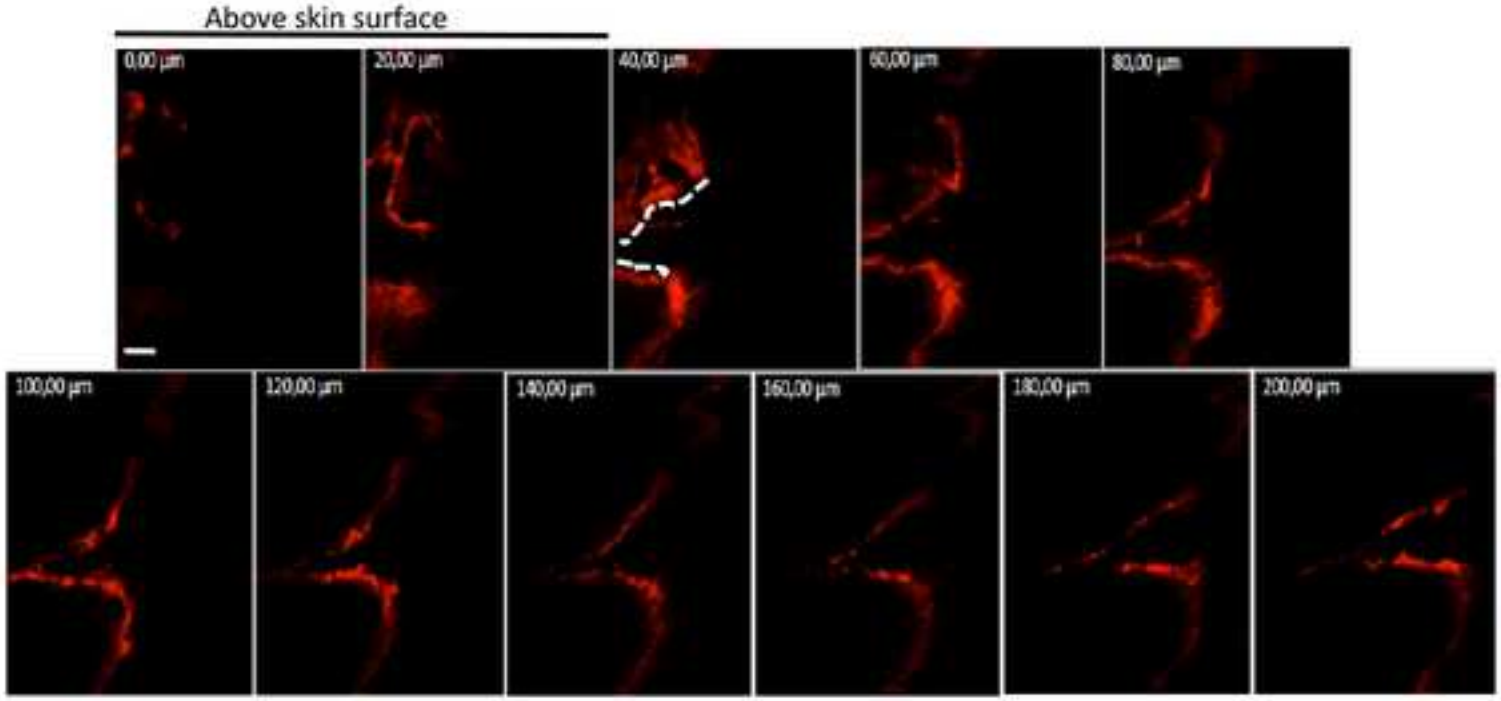

Figure 8

Click here to download high resolution image

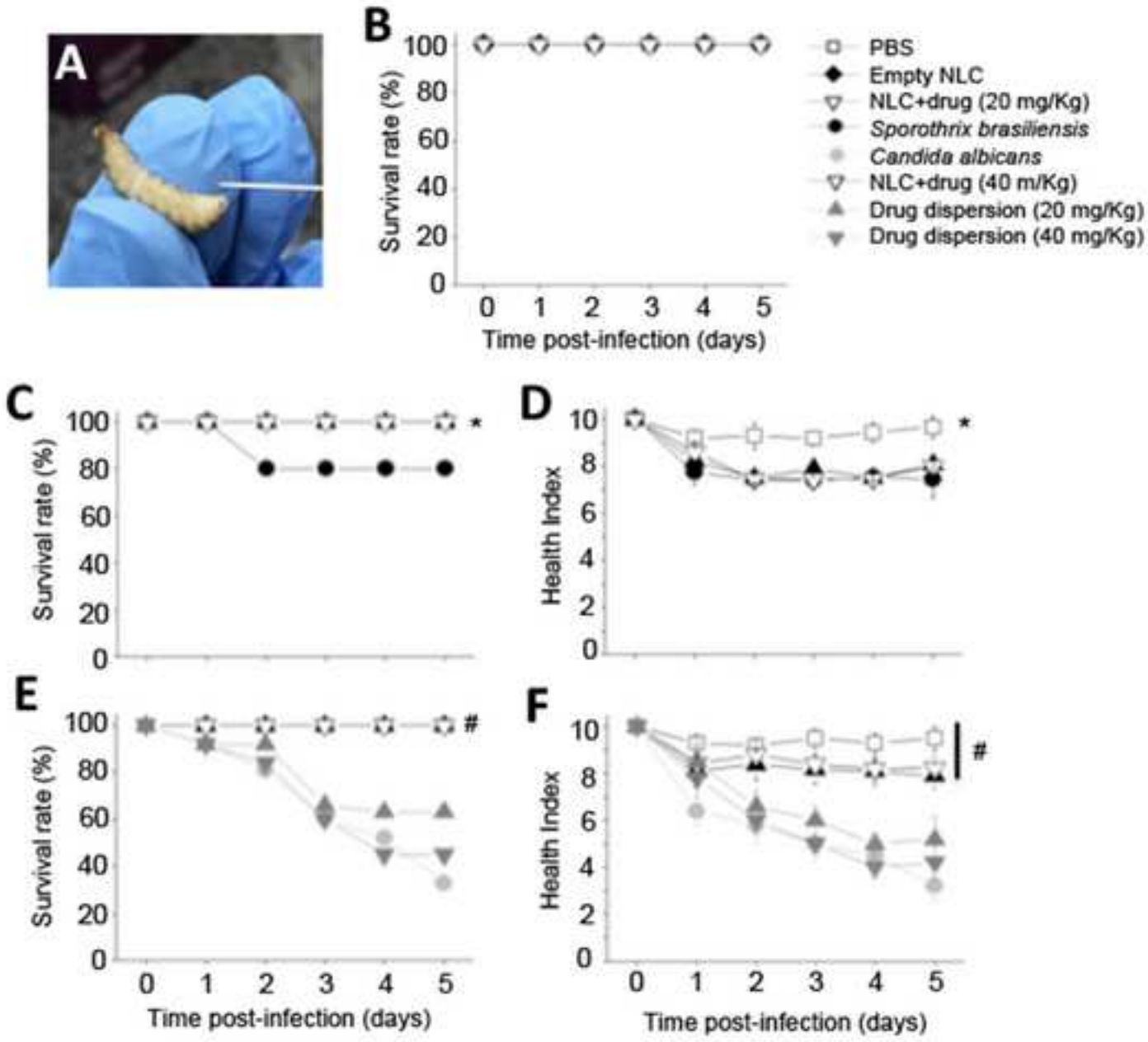

Table 1. Physicochemical properties of NLC. Data represents average ± standard deviation of 3 formulation batches.

Formulations and variables	Size (nm)	PDI	Zeta potential (mV)
Solid:liquid lipid ratio (w/w)			
7:3	309.7±2.7	0.25±0.01	-18.4±0.8
5:5	225.5±14.5	0.19±0.03	-17.3±1.3
3:7	349.1±42.8	0.38±0.02	-17.9±0.7
Surfactant concentration			
Tween (1.5%), Span (1.5%)	289.6±8.1	0.33±0.03	-20.6±0.3
Tween (1,5%), Span (3%)	294.3±8.6	0.32±0.02	-18.9±0.1
Tween (3%), Span (1.5%)	250.0±5.9	0.24±0.03	-17.6±0.7
Tween (3%), Span (3%)	216.3±2.5*	0.20±0.01*	-17.4±1.9

* $p < 0.05$ compared to the formulation containing Tween and Span at 1.5%.

Table 2. Thermogravimetric analyses of selected samples.

Sample	Melting band	T_{peak}	ΔH (mJ/mg)
Glyceril behenate	67-73	70	123
Tricaprilyn	na	na	na
Itraconazole	166.6	169	79.3
NLC	58-65	63	57.5
NLC 1%	56-62	60	34.2

PM: Physical mixture

NLC: Unloaded NLC

NLC 1%: Itraconazole-loaded NLC

na: not applicable

Table 3. Minimum Inhibitory Concentration (MIC) and Minimum Fungicidal Concentration (MFC) of itraconazole (in solution - ITC and loaded-nanocarrier - NLC), Fluconazole (FLC) and Amphotericin B (AMB) against *Sporothrix brasiliensis* and *Candida albicans*. MIC and MFC are expressed in μg/mL.

Strains	**NLC**		**ITC**		**FLC**		**AMB**	
	MIC	*MFC*	*MIC*	*MFC*	*MIC*	*MFC*	*MIC*	*MFC*
Sporothrix brasiliensis Sb54	0.25	32	0.12	>16	8	>64	0.5	2
Candida albicans SC5314	1	>128	0.12	>16	0.25	>64	0.25	8

Supplementary video1

Click here to download Supplementary Material: video_skin.mov

Suppmentary Table 1. Health index of *Galleria mellonella* larvae

Health index

Category	Description	Score
Activity	No movement	0
	Minimalmovementonstimulation	1
	Move whenstimulated	2
	Move withoutstimulation	3
Cocoonformation	No cocoon	0
	Partialcocoon	0.5
	Fullcocoon	1
Melanisation	Black larvae	0
	Black spots on brown larvae	1
	≥3 spots onbeigelarvae	2
	<3 spots onbeigelarvae	3
	No melanisation	4
Survival	Dead	0
	Alive	2